Application of Duncan-Chang Model on the Numerical Analysis Considering the Clay Heterogeneity

Wei Wang(✉), Peiling He, Binghua Zhao, Aiyu Hu, and Jibin Shang

Nanjing Institute of Technology, 1 Hongjing Street, Nanjing, China
wwll77ll4@163.com

Abstract. More generally, the clay specimen is regarded as the homogeneous body in the process of numerical analysis. In effect, the clay is heterogeneity. Aim to study the evolution features of shear stresses and rotation angles of major principal stresses at out of shear band during early loading state based on clay actual mesostructures using the Duncan-Chang theory, the actual mesostructures were taken into consideration when the clay numerical model was constructed. Through the microscope, the original image which included the clay skeleton and the pores before loading was captured. Then, the Otsu's method was used to convert the image captured into the binary one for identifying the exact boundaries between the skeleton and the pores. The binary image, in which white areas were called the skeleton while the black ones were the pores, was transformed into the vector diagram which was the input document for the finite element software. So, the 2D model with clay actual mesostructures was established based on the vector-graph. Meanwhile, the model parameters used in the 2D model were given by the triaxial compression test. Then, the numerical analysis was performed for simulating the unconfined compressive test. The results show that the actual model can not only reveal the evolution features of internal shear stresses and rotation angles of major principal stresses at "points" located in skeleton from the mesoscopic but also depict the evolution curves of Mises stresses along the paths.

Keywords: Soil mechanics · Duncan-Chang model · Actual mesostructures Numerical analysis

1 Introduction

In recent years, some progresses have been presented on the clay heterogeneity in the field of soil mechanics. Many geotechnical researchers don't take the soil as a simple macro-body but a structural body with complex mechanical properties given the combination of the mesoscopic research on soil structures and the macro-properties of soil materials [1–3]. Specially, researching the distribution and transmission of contact stresses between soil particles located in the skeleton needs us to discuss deeply the mechanical response from the mesoscale. That is to say, the research of soil mesostructures [4, 5] will help us to understand the microscopic evolution features of

A. Zhou et al. (Eds.): GSIC 2018, *Proceedings of GeoShanghai 2018 International Conference: Fundamentals of Soil Behaviours*, pp. 929–937, 2018.
https://doi.org/10.1007/978-981-13-0125-4_103

shear stresses and rotation angles of major principal stresses [6, 7]. Moreover, it would be helpful to analyze the fundamental cause of landside and debris flow.

As we know, soil engineers used the DEM to simulate soil specimens with spherical particles. Due to limitations of experiment sets, DEM numerical tests (Ding et al. (2013) [8], Mahmood et al. (2011) [9], Pena et al. (2007) [10], Pietruszczak et al. (2013) [11]) show greater advantages for studying the relationship between mesostructures and macroproperties of soil. Nicot et al. (2015) [12] firstly performed the numerical simulations of granular materials subjected to proportional strain loading paths using the DEM and secondly corroborated the DEM results with two micromechanical models. Zhang et al. (2016) [13] conducted a series of biaxial tests based on DEM and investigated the variation of soil-rock mixture's mesostructures during tests. Sun et al. (2010) [14] proposed that the inter-particle forces of granular matter were transmitted through heterogeneous chain architecture and the force chains would display different response as external loading varies. While, the numerical models used in the above researches were generated randomly and they didn't reflect the actual mesostructures of geomaterials. It is believed that the models with random aggregate structure cannot exactly represent the actual geomaterial inhomogeneities and microstructures. Moreover, the particles adopted in the models were assumed to be rigid, which was different from the actual geomaterials.

So, in order to quantitatively study the correlation between the actual mesostructures and macro-properties of soil, we firstly realized the elastic numerical analysis of the cement soil based on the 2D model with actual mesostructures [15]. In this paper, the air-dried clay was prepared for the unconfined compressive test. We assume that the small amount of moisture has little or no effect upon the mechanical properties of the clay. Then, the 2D numerical model including actual mesostructures of the undisturbed clay was established and analyzed using the Duncan-Chang theory. Based on it, we explored the evolution of shear stresses and rotation angles of major principal stresses at out of shear band of the air-dried clay during the application of loads.

2 Establishment of Numerical Model

Using the axial symmetry principle, the cylindrical specimen of the air-dried clay, which was commonly about 39.1 mm in diameter and 80 mm in length, was broken into two half-cylindrical specimens. The local region at out of the shear band located in the axisymmetric section including clay mesostructures was captured by the CCD (Charged-coupled Device) camera before applying the unconfined compressive test. According to the grayscale of the original image, the threshold value of the image was 0.1775 calculated by the Otsu's method that describes the probability of variance between target and background. The distribution characteristic about the skeleton and the pores that form the inhomogeneity of the clay were identified, in which white areas were called the skeleton while the black ones were the pores. After detecting the irregular edges between the pores and the skeleton through the edge detection algorithm, the edge detection image was transferred into the vector diagram using vector graphics software CoreDRAW. Finally, the 2D numerical model with the clay mesostructures was established successfully. According to the complexity of the

model, the Adaptivity technique was used to mesh it in the numerical software. (Note: The Adaptivity technique, which is supported by the software ABAQUS, is used to deal with the grids distorted highly. In this paper, we adopted the Arbitrary Lagrangian Eulerian adaptive meshing). Figure 1 shows the establish process of the 2D numerical model.

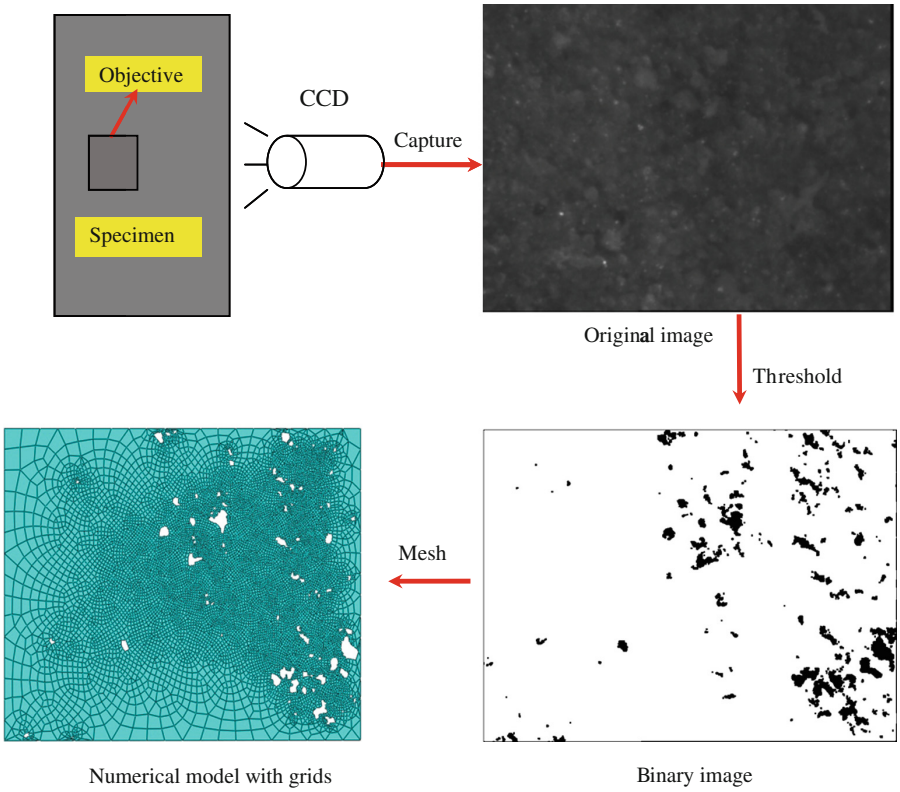

Fig. 1. The establish process of 2D numerical model

3 Determination of Model Parameters and Boundary Conditions

In order to analyze the numerical model with clay mesostructures, the numerical model parameters were needed. Hence, the material parameters of the clay model used in Duncan-Chang theory, which are shown in Table 1, were determined through the triaxial compression test such as: cohesion, friction angle, etc. In this paper, we are concerned the results from the macroscopic test and the meso-numerical simulation. So, on the one hand, we acted on the unconfined compressive test with half-cylindrical specimen; on the other hand, we also simulated the unconfined compressive test using

the model with clay mesostructures. In the process of simulating, the bottom boundary of the model was regarded as the fixed support and the loadings were acted on the upper boundary of the model. Additionally, considering the rationality of the model and the limitation of the meso-image, the break point at the boundary and the tiny pores in the model were all ignored.

Table 1. Numerical model parameters of the clay.

K	n	R_f	c/kPa	$\varphi/(^{o})$	G	D	F	K_{ur}	Pa/kPa	$\Delta\varphi/(^{o})$
100	0.8	0.588	50.04	28.51	0.281	1.2	0.031	150	100	0.02

4 Numerical Analysis and Results

The published literatures prove that researching stress characteristics of soil in the initial state using Duncan-Chang theory are more accurate than other constitutive theories. So, in this paper, the external loads were added to 50 kPa on the numerical model, in spite of the failure load of the air-dried clay was 240 kPa obtained from the unconfined compressive test. In order to discuss the evolution of shear stresses and rotation angles of major principal stresses at out of the shear band, two typical elements shown in Fig. 2 were selected. The first element labeled No. 129 element was located next to the boundary of a large pore. The second one labeled No. 6450 element was situated on the place away from pores, whose stress value was about the same as the

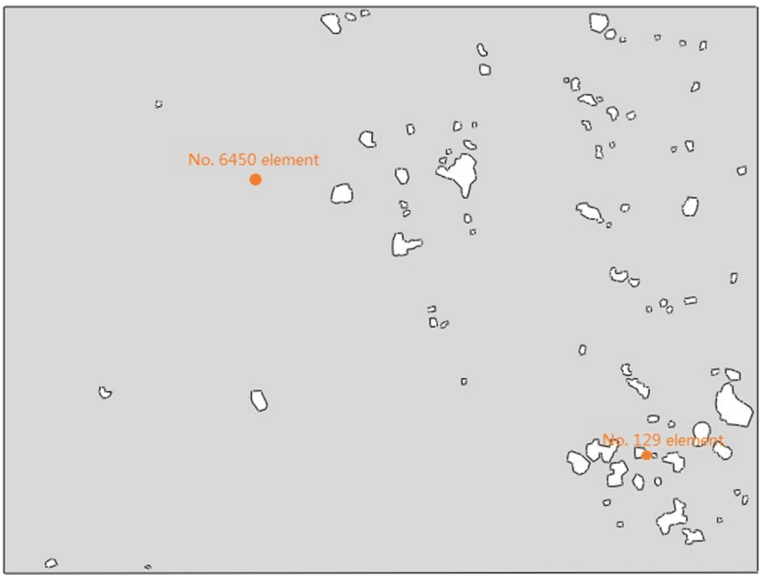

Fig. 2. Two typical elements selected

external load. There are a few meaningful results from the quantitative research on the shear stresses and rotation angles of the two elements below.

From the numerical results of the model, the magnitudes of the shear stresses, the major principal stresses and the minor principal stresses at the two elements all could be directly obtained. Thus, using the following equation, the rotation angles of the major principal stresses could be found at every loading level.

$$\tau = \frac{\sigma_1 - \sigma_3}{2} \sin 2\theta \tag{1}$$

Further, the normal stresses of the two elements were also found using the following equation.

$$\sigma_n = \frac{\sigma_1 + \sigma_3}{2} + \frac{\sigma_1 - \sigma_3}{2} \cos 2\theta \tag{2}$$

Next, based on the Mohr theory, the shear strength (τ_f) of the two elements could be drawn easily using the normal stresses obtained above. $\tau_f = c + \sigma_n \tan \varphi$ (Here, c is the cohesion and φ is the friction angle) Fig. 3 (a) and (b) are the evolution curves of angles inclined to the direction of the major principal plane and the changing curves of shear stresses and shear strengths of the two elements along the increasing loads respectively. As shown in Fig. 3, we can learn that the rotation angles of two elements are gradually increased with the increasing loading. It is knowable that every element in the model is interrelated. It also indicates the same tendency for the angles when the loading is applied from 0 to 50 kPa, although there are different initial angles and different slopes. This suggests that the balance between external forces and internal forces is achieved through congregate particles rotating in this state. Moreover, the rotation speed of the angle labeled No. 129 element is increased rapidly. Obviously, the final value is four times larger than the initial value, which illustrates that the shape of particles might change so as to resist increasing loads. It may be the reason that the element labeled No. 129 element at the boundary of a large pore has not enough constraints leading to rotation angle increasing. Furthermore, for the labeled No. 6450 element away from the pores, the rotation angle is increasing along the loads and the slope of the curve is less than the slope of the one labeled No. 129 element. Because there are no pores around the congregate particles at this mesoscopic level, the evolution feature of rotation angles located in the skeleton is same to the macroscopic properties of soil specimen. Above all, the congregate particles at the elements reorganized undoubtedly and possessed new shear strengths to resist external loads. Additionally, Fig. 3 also describes the relationship between shear stresses and shear strengths of the same element. The shear strengths are evidently larger than the shear stresses, which tell us the congregate particles can be still subjected to loads in initial state. At the same time, both shear stresses and shear strengths of elements keep increasing along the loading.

Figure 4 indicates the change rules of Mises stresses along different paths. Figure 4(a) shows the path that locates in the region away from pores. The Mises stress is fluctuation from the start point to the end point, which quantitatively demonstrates

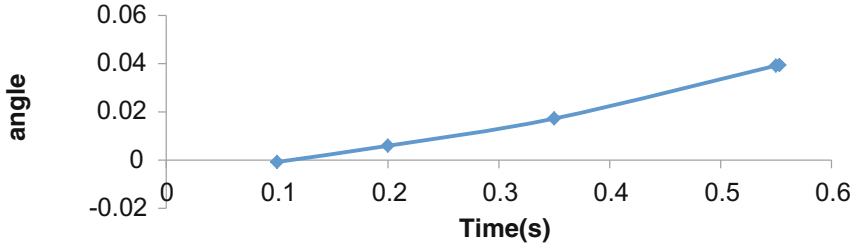

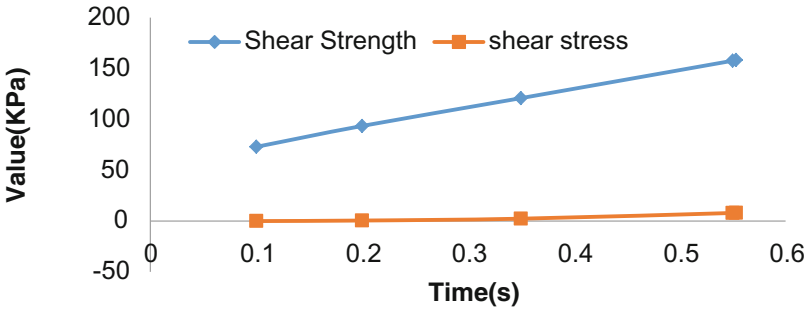

(a) 129 element

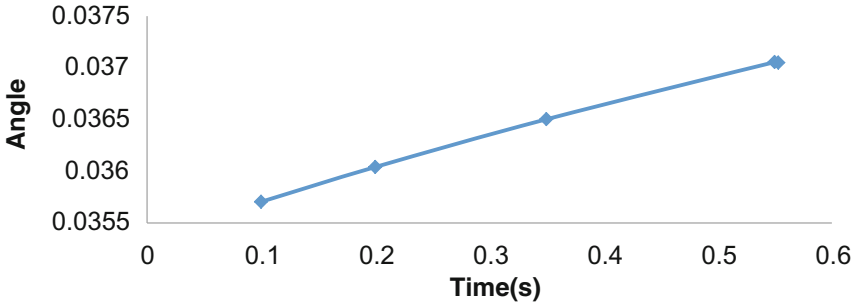

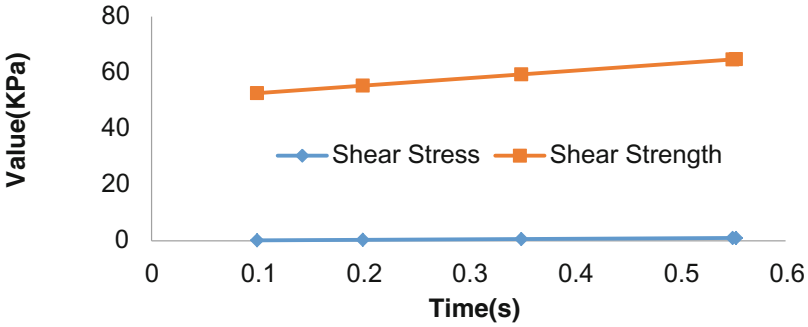

(b) 6450 element

Fig. 3. The evolution of shear stresses and rotation angles of principal stresses

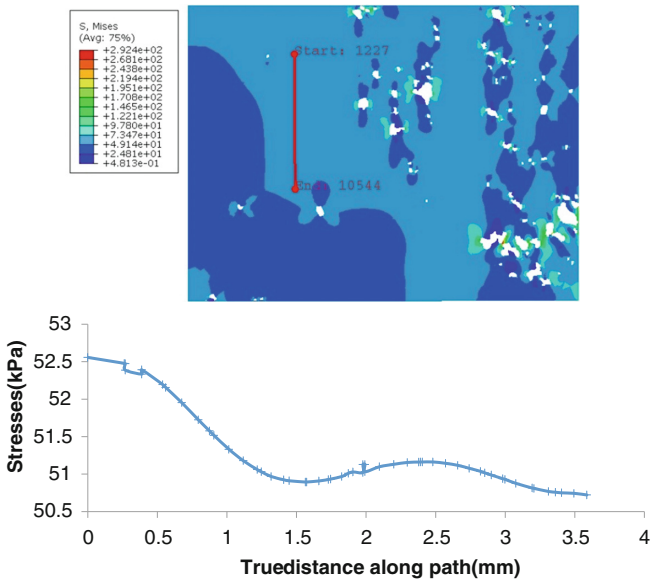

(a) Path away from pores

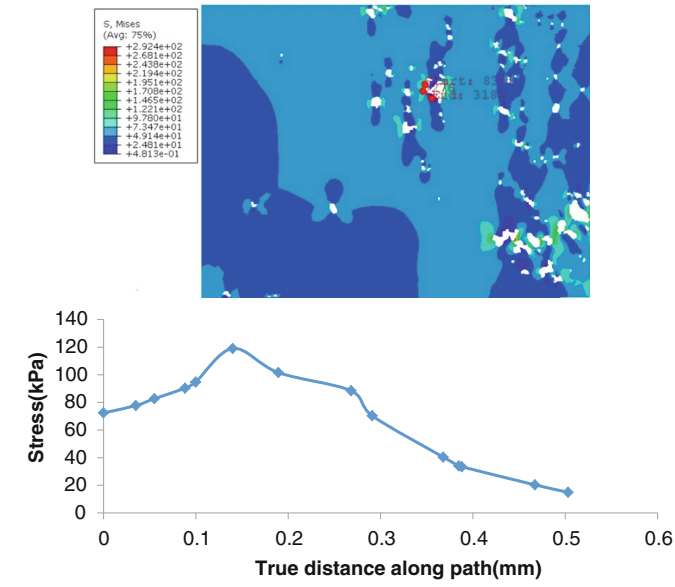

(b) Path surrounding pores

Fig. 4. Stress paths and evolution curves of Mises stress along path

the complexity of the internal stress of clay. However, the fluctuation range of the Mises stress is small and the average value is about 51.5 kPa, approximately equal to the external load, which is similar to the properties of homogeneous body. We believe that the contact stress located in the region reflects the macroscopic mechanical properties of clay specimen under the stable state. Figure 4(b) describes the path that is located next to the pores. The Mises stress fluctuates remarkably. Specially, the Mises stress is high on the side of the pore and the stress located in the bottom of the pore is less than the stress at the topside of the pore. The peak stress, which is about 130 kPa, is called the strong contact stress, while other stresses around it are weak contact stress. Obviously, the contact stress network is scattered throughout the clay specimen. The strong contact stress often occurs next to the pores, which is surrounded by the weak contact stresses. The rupture of the strong contact stress is the precondition of clay destruction.

5 Conclusions

Actually, the image processing technology can be used as the effective measurement to get quantitative information based on clay mesostructures. Furthermore, it is feasible that the numerical model with clay mesostructures is analyzed using the Duncan-Chang theory. It makes sense that particles rotation under the loading results in the changing of the shape of clay particles. And, the magnitude and the speed of rotating reply on the position of congregate particles. The slope of angle curves located away from pores is much smaller than other slopes of angle curves.

Moreover, there is a tight connection between strong contact stress and pores in dry clay. That is demonstrated that pores, especially large pores, play a significant role in the analysis of meso-stresses. As a result, the clay baring external loads depends on the stable network of contact stress formed.

References

1. Sekiguchi, H., Ohta, H.: Induced anisotropy and time dependency in clays. In: Proceedings of 9th ICSMFE, pp. 229–238. SSMFF, Tokyo (1977)
2. Xie, D.Y., Yao, Y.P., Dang, F.N.: Advanced Soil Mechanics. Higher Education Press, Beijing (2008)
3. Baudet, B., Stallebrass, S.: A constitutive model for structured clays. Geotechnique **54**(4), 269–278 (2004)
4. Chang, C.S., Hicher, P.Y.: An elastic-plastic model for granular materials with microstructural consideration. Int. J. Solids Struct. **42**(14), 258–4277 (2005)
5. Goodarzi, M., Rouainia, M., Aplin, A.C.: Numerical evaluation of mean-field homogenization methods for predicting shale elastic response. Comput. Geosci. **20**(4), 793–807 (2016)
6. Yang, L., Wang, C.G., Zhang, D.: Distribution and evolution of pore structure in 2D granular materials under biaxial compression. Chin. J. Geotech. Eng. **37**(3), 494–503 (2015)
7. Liu, S., Shao, D., Shen, C., Wang, Z.: Microstructure-based elastoplastic constitutive model for coarse-grained materials. Chin. J. Geotech. Eng. **39**(5), 777–783 (2017)

8. Ding, X.L., Zhang, H.M., Huang, S.L., Lu, B., Zhang, Q.: Research on mechanical characteristics of unsaturated soil-rock mixture based on numerical experiments of mesostructure. Chin. J. Rock Mech. Eng. **31**(8), 1553–1566 (2012). Yanshilixue Yu, Gongcheng Xuebao
9. Mahmood, Z., Iwashita, K.: A simulation study of microstructure evolution inside the shear band in biaxial compression test. Int. J. Numer. Anal. Meth. Geomech. **35**(6), 652–667 (2011)
10. Pena, A.A., Garcia-Rojo, R., Herrmann, H.J.: Influence of particle shape on sheared dense granular media. Granular Matter **9**(3–4), 279–291 (2007)
11. Pietruszczak, S., Guo, P.: Description of deformation process in inherently anisotropic granular materials. Int. J. Numer. Anal. Meth. Geomech. **37**(5), 478–490 (2013)
12. Nicot, F., Sibille, L., Hicher, P.Y.: Micro-macro analysis of granular material behavior along proportional strain paths. Continuum Mech. Thermodyn. **27**, 173–193 (2015)
13. Zhang, H.Y., Xu, W.J., Yu, Y.Z.: Numerical analysis of soil-rock mixture's meso-mechanics based on biaxial test. J. Cent. South Univ. **23**(3), 685–700 (2016)
14. Sun, Q.C., Jin, F., Wang, G.Q., Zhang, G.H.: Force chains in a uniaxially compressed static granular matter in 2D. Acta Physica Sinica **59**(1), 30–37 (2010)
15. Wang, W., He, P.L., Zhang, D.H.: Finite element simulation based on soil mesostructues extracted from digital image. Soil Mech. Found. Eng. **52**(1), 17–22 (2014)